Global NEST Journal, Vol 27, No 1, 06903

Influence of the injector nozzle on hydrogen-powered juliflora biodiesel in HCCI engines: a surface response methodology approach

Venkatesan S.[a], Raghu P.*[, b] and Nagaraj M.[c]

[a]Research Scholar, Department of Mechanical Engineering, Sri Venkateswara College of Engineering, Pennalur, Sriperumbudur–602 117, Tamilnadu, India.

[b]Department of Mechanical Engineering, Sri Venkateswara College of Engineering, Pennalur, Sriperumbudur–602 117, Tamilnadu, India.

[c]Institute of Agricultural Engineering, Saveetha School of Engineering, Saveetha Institute of Medical and Technical Sciences (SIMATS), Chennai, 602 105 India.

Received: 18/10/2024, Accepted: 03/12/2024, Available online: 19/12/2024

*to whom all correspondence should be addressed: e-mail: praghu@svce.ac.in

https://doi.org/10.30955/gnj.06903

Graphical abstract

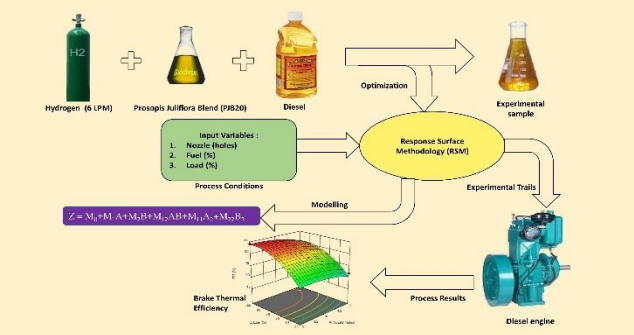

Abstract

Hydrogen is a possible future energy carrier due to its production potential from renewable resources and compatibility with existing diesel engines with minor changes in dual-fuel mode. Various studies have explored modifying engine structure, optimizing operating conditions, adjusting engine parameters, and using exhaust gas catalysts to safely and efficiently integrate hydrogen and other gaseous fuels. This study examines the improvement and emission phenomenon of Homogeneous Charge Compression Ignition (HCCI) engines using diesel, biodiesel, and a blend of Juliflora Biodiesel (B20) with hydrogen at 6 LPM in dual-fuel combinations. The HCCI engine's versatility in utilizing diverse fuels, including hydrogen, biofuels, diesel, and gasoline, is a significant advantage. In contrast, injector nozzle number is limited in research, particularly in gaseous fuel. This study employs gaseous fuel to evaluate how nozzle holes impact engine performance and emissions. The objective of this research is to experiment with an HCCI engine in dual-fuel mode by varying the injector nozzle holes (3, 4, and 5) to identify the optimal fuel mix and operating conditions that enhance performance and reduce emissions. Our primary fuel was Prosopis Juliflora Biodiesel (B20) with hydrogen use as a secondary fuel introduced through the inlet manifold. The experimental results indicated that a 4-hole nozzle at 50% load (B20 + H_2 @ 6 LPM) provided superior atomization and increased brake thermal efficiency, along with reduced HC, CO, and smoke opacity compared to the 3 hole and 5 hole nozzles. Response surface methodology confirmed that these experimental findings align with optimized parameters. Therefore, we recommend using a 4-hole nozzle for the B20 + H_2 blend at 6 LPM and 50% load to achieve enhanced performance and emission reductions in HCCI engines compared to 3-hole and 5-hole nozzles.

Keywords: Hydrogen blending, injector nozzle, optimization, response surface methodology (rsm), engine efficiency, emission control

1. Introduction

The automotive sector faces the greatest hurdles in reducing greenhouse gas emissions and fossil fuel consumption. In this environment, biodiesel and hydrogen are emerging as mitigating options. Sustainable biodiesel is made from edible oils like soybean or canola and inedible oils like recycled cooking oil or algae. Using a catalyst, transesterification produces FAME and glycerin from fat or oil and methanol or ethanol. Similar to petroleum diesel, biodiesel can be blended or run alone in diesel engines. It employs renewable resources, minimizes greenhouse gas production, and depends less on fossil fuels, making it greener. Biodegradable and less polluting than diesel. Gerhard Knothe *et al.* (2024), (Soni *et al.* 2024), (Krishna Shrivastava, *et al.* 2021), (Preechar Karin *et al.* 2022), (Bhaskor J Bora *et al.* 2022), Mittelbach, M., & Schober, S. (2003) Santos, M. C., & Oliveira, F. (2011).

Hydrogen, on the other hand, is claimed for its clean characteristics of burning to provide only water vapor as its by-product. In this context, homogeneous charge compression ignition (HCCI) engines have positioned themselves as one of the most promising technologies (Tutak, *et al.* 2023), (Swarup Kumar Nayak 2019), (Ram Narayan Bhagat *et al.* 2023).

Unlike traditional internal combustion engines, ignition in an HCCI engine occurs by compression heating of a homogeneous mixture of air and fuel, leading to more uniform combustion. So, thermal efficiency can be increased and NOx and PM emissions reduced. On the other hand, HCCI performance is very sensitive to fuel properties and tight control over combustion parameters. It is because injector nozzles have been one of the critical factors in the design process for the optimization of HCCI engine performance. The geometry of the injector nozzle, such as the hole size, spray angle, and injection pressure, significantly influences the fuel atomization and distribution process inside the combustion chamber. Therefore, these factors have a huge influence on the formation of air-fuel mixtures, the efficiency of combustion, and the characteristics of emission. (Saravanan *et al.* 2008), (Khan *et al.* 2012), (Deheri *et al.* 2020), (Gandhi Pullagura *et al.* 2024), (Osama Khan *et al.* 2024), (Karagöz *et al.* 2016), (Su Wang *et al.* 2023), (Avadhoot Mohite *et al.* 2024). Seyyed Hassan Hosseini *et al.* (2023) did a review on the behavior of hydrogen or hydrogen-containing gaseous fuels in dual fuel mode within diesel engines. Their findings indicate that using hydrogen alone does not necessarily improve the efficiency regarding combustion and emission phenomenon. However, they propose that modifying the engine structure, optimizing operating conditions, adjusting engine parameters, and exploring alternative gaseous fuels could lead to safer and more efficient utilization, potentially incorporating exhaust gas catalysts. They recommend further research to explore these approaches and enhance the application of gaseous fuels in diesel engines.

Longlong Xu *et al.* (2022) explored hydrogen as a clean, renewable alternative fuel by developing and validating a combustion mechanism for diesel/hydrogen dual fuel engines. They examined how pilot and main injection affected combustion and emissions in these engines using three-dimensional numerical models. Researchers substituted diesel with a combination of 70% mole fraction n-decane and 30% mole fraction α-methylnaphthalene. Combustion dynamics in diesel/hydrogen dual fuel engines were modeled using n-decane, α-methylnaphthalene, NO_x, PAH, soot, and H_2/C_1-C_3 sub-mechanisms.

Parimi K.B. *et al.* (2023) The study evaluates how a blend of Kusum seed biodiesel (KSOBD20) enriched with hydrogen compressed natural gas (HCNG) affects the performance, combustion, and emissions of a compression-ignition engine. HCNG was introduced at varies rates of 5 LPM, 10 LPM, and 15 LPM, with injection pressures varying from 180 bar to 240 bar. Results indicate that adding HCNG improved efficiency and reduced BSFC, particularly at higher injection pressures. Parameters such as net heat release rate (NHRR) and cylinder pressure (CP) also showed enhancements. Emissions of smoke, HC and CO decreased, while NOx emissions remained stable. Optimal engine performance was accomplished with KSOBD20 + 15 LPM HCNG at an injection pressure of 240 bar suggesting potential efficiency improvements and emissions reductions in sustainable fuel applications. Ibham Veza's research on Response Surface Methodology (RSM) underscores its role as a statistical tool for optimizing process variables through designed experiments, drawing from principles in Design of Experiments (DOE). DOE is integral to applied statistics, involving planning, conducting, analyzing, and interpreting controlled tests to understand factors affecting parameter values. Despite RSM's potential to detect and optimize engine emissions and performance, there remains a notable absence of comprehensive reviews focusing specifically on its application for biofuels in Internal Combustion Engines (ICEs). This gap highlights the need for dedicated review articles that delve into RSM's application in optimizing engine performance and emissions using biofuels. Such reviews would critically evaluate RSM's efficacy, identify research gaps, and emphasize its potential in advancing ICE optimization with biofuels for sustainable energy transitions.

Fakkir Mohamed M. *et al.* (2021) This study focuses on Optimization of biodiesel performance and emissions in a variable compression engine utilizing RSM and Box-Behnken Design. The experiment involved 15 runs varying blend composition (B), compression ratio (CR), and engine load (L). Responses such as BTE, BSFC, HC, and CO and NOx were assessed. RSM models were used to determine optimal parameters, achieving highest desirability for BSFC (1.0) and BTE (0.91), and minimizing NOx (0.95), HC (0.68), and CO (0.55). With blend B10, CR 16:1, and a 5 kg load, the composite desirability was 0.79 with validation confirming close agreement between model predictions and experimental results. Patrick Rorimpandey *et al.* (2023) investigates the interplay between diesel-pilot and hydrogen (H_2) jets in a compress-ignition engine simulation. The researchers tested several injection sequences, timings, and ambient temperatures (780-890 K) using two single-hole injectors in a visually viewable constant-volume combustion chamber (CVCC). They found that injecting diesel-pilot before H_2 requires a longer delay for ignition due to the cooling effect of burnt diesel products. Injecting H_2 before diesel-pilot affects combustion spread through the H_2 jet, influencing ignition timing and mixture conditions. Lower ambient temperatures increase combustion variability, primarily due to lean-out effects in the diesel-pilot combustion process.

Sushrut S. Halewadimath *et al.* (2023) applied the RSM with the effect of flow rates on performance, emissions, and combustion phenomenon of a dual-fuel engine running on biodiesel, PG, and hydrogen. The novelty is the optimization of the fuel rates with various NeOME fuel

blends with hydrogen. All RSM models turned out to be significant with a confidence limit of 95%. The best flow rates of fuel that gave the optimum for biodiesel, producer gas and hydrogen, with best responses of BTE, HSU smoke, HC, CO, NOx, Pmax, ID, and HRR. Sharma, examines soya and soya-ethanol blends for performance and emission characteristics in an unmodified compression-ignition engine using the response surface methodology. Of interest were the fuel blends, speed of the engine, rate of air flow, and the engine load. The ideal test parameters for an 8% soya blend in dual-fuel mode are 1486 RPM, 49.5 mm air flow, and 6.27 kg load obtained a brake thermal efficiency of 24.29%, volumetric efficiency of 68.53%, and emissions of 0.0715% of CO by volume, HC of 51.6 ppm, and NOx of 1080.2 ppm.

In 2015, Najafi applied the approach of desirability within the framework of response surface methodology for optimization in view of minimizing emission and maximize performance metrics. A DoE framework, whose roots stemmed from RSM, was used in this study. The desirability approach applied to find an optimum setting of the engine. Different biofuel-gasoline blends trended similarly to those of gasoline with considerable improvement in emission characteristics. At 3000 rpm, the engine performed at its best using a 10% bioethanol with 90% gasoline blend (E10).

Real experiment findings and R^2 actual values that illustrate the relationship between optimization outputs and real experiments matched well. The optimal component concentration was 65.5 vol.% diesel, 23.1 vol.% n-butanol, and 11.4 vol.% cotton oil. Compared to diesel fuel, braking torque, brake power, BTE, and BMEP fell but BSFC increased in engine performance tests. NOx, CO, and HC emissions dropped 11.33%, 45.17%, and 81.45% Atmanli *et al.* (2020) and Sagari *et al.* (2020). Rajesh *et al.* (2022) observed a significant increase in the SFC of the biodiesel that contained 18% (BD18) polymer oil when it was loaded with 4.4 kg, 9.03 kg, and 12.6 kg. With a plastic fuel addition of 6% (BD6) at 17.04 kg, it had a high specific fuel capacity (SFC). In every instance, the pure diesel shown a significant SPC, which was then followed by the addition of 12% (BD12) polymer oil.

Rajesh *et al.* (2022) discovered the pyrolyzed PP based polymer oil and pure diesel were tested. Using 4% plastic oil, the indicated power differs by approximately 0.01 kW at a load of 0.04 kg and rises to approximately 0.02 kW at a weight of 17.04 kg. At a weight of 0.04 kg, the braking power for 4% plastic oil is 0.02 kW, which is the same as the BP for diesel operation under identical conditions. In comparison to diesel, the braking power for 4% plastic oil varies by approximately 0.02 kW under higher load conditions. Allasi *et al.* (2023) found that influence of the synthesized CeO2 and ethanol on the biodiesel made from neem oil was investigated using a number of different metrics, including performance, emission, and combustion. Hybrid cerium oxide nanoparticles and ethanol exhibit superior performance due to improved atomization and oxygen buffering. Prabhu Kishore *et al.* (2024) employs high-reactivity jatropha oil combined with diesel and low-reactivity 1-hexanaol. Different fuel approach increased BTE by 36.83% and decreased BSFC by 19.48%. The hazardous pollutants smoke, UHC, CO, and CO_2 by 55.86%, 30%, 52.33%, and 46.3%. Ganesh botla *et al.* (2024) Furthermore, optimization studies have been conducted to determine the best operating parameters for thermal cracking HDPE waste polymers into valuable products. RSM improves independent variables to boost value-added product yields. Prathiba Rex *et al.* (2024) Focussed on polypropylene waste (PPW) and polyethylene terephthalate (PETW) were pyrolyzed in a semi-batch reactor at 500°C for the studies. Lastly, waste plastics pyrolysis is a suitable option to produce diesel-like fuel. Because biodiesel typically has a fuel with higher flash point, higher pour point and greater calorific value, it is possible to get the best possible performance from a dual fuel engine by using biodiesel as the fuel

This study aims to examine the effects of number of nozzle hole on the performance of dual engines using blends of PJB20 with 6 LPM, diesel and PJB20. By employing response surface methodology, the research systematically varies nozzle parameters and operating conditions to identify best possible configurations. RSM is a influential statistical tool that facilitate the modeling and analysis of complex interactions between multiple variables, facilitate the optimization of process parameters with a reduced number of experiments.

2. Experimental procedure

The experimental utilizes a single-cylinder diesel engine, depicted in **Figure 1** below, and designed with air-cooling and a vertical orientation, employing direct injection technology. It produces up to 5.5 kW at 1500 rpm. The engine has a 17.5 compression ratio, 230 bar injection pressure, and 23.4^0 before top dead center injection timing. Injector nozzles are available in configurations with 3 holes, 4 holes, and 5 holes. **Table 1** describes the complete specification of the engine. A dynamometer is connected to the engine for load measurement. On the intake side, the setup includes an air heater, an anti-pulsating drum, and an air temperature monitoring device. The exhaust system is equipped with components such as an gas analyzer, an exhaust temperature indicator, and a smoke sampler. Furthermore, an independent apparatus measures the consumption of biodiesel blend fuel accurately. In a dual-fuel setup, there are normally diesel engines that make use of one type of fuel being injected into combustion chamber is PJB20, while the second fuel is introduced into the intake system, such as hydrogen 6 lpm. After bringing the 180 bar pressure of hydrogen gas held in a cylinder down to 1 bar with a pressure regulator, the gas was fed to the injector via a non-return valve, and the flow meter measured out the amount of gas. This was also injected into the inlet manifold of the engine by the injection of hydrogen. The test rig is equipped with a 64-bit data acquisition (DAQ) device to capture detailed data on crank angle and cylinder pressure. Engine loading is facilitated using a swinging field electrical dynamometer.

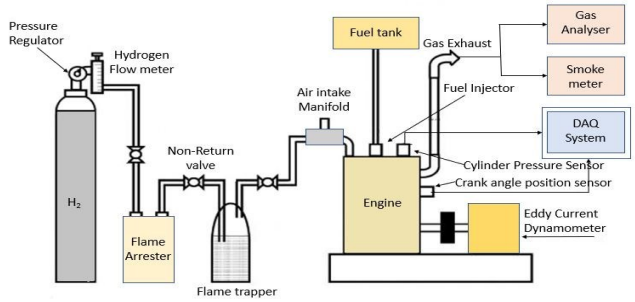

Figure 1. Experimental setup

Transesterification is a process involving Prosopis juliflora seed oil for biodiesel production, using methanol and potassium hydroxide, acting as catalysts. The ratio of methanol to seed oil, the concentration of the catalyst, the temperature conditions, and the reaction time are the basic process parameters. The optimal conditions for the process are 4% NaOH for 1.5 liters of the oil at a temperature of 80°C for 80 minutes with 15% methanol, producing 82.08% biodiesel. After the reaction, glycerine settles at the bottom, and at the top, biodiesel is collected. Water is used to wash biodiesel for the removal of residual glycerine and is then heated up to 100°C to evaporate the water content. Properties of diesel, PJB20, and hydrogen are summaries as follows: It, therefore, possesses varying characteristics compared to PJB20, whereby diesel has: density: 840 kg/m³ at 20°C, calorific value: 43,000 kJ/kg, and viscosity: between 2.5 to 3.2 cSt. The flash point is 65°C, and the fire point is 78°C, while its cetane number lies in the range of 45 to 55. It has higher density of 839 kg/m³ at 20°C compared to PJB20, with a calorific value of 41,769 kJ/kg and viscosity of 2.854 cSt. On the contrary, flash point is 82°C with a fire point of 90°C and a cetane number of 45. On the other hand, hydrogen gas has a flame velocity of 265 to 325 with a calorific value of 120.5 MJ/kg and a density of 0.0899 g/L. It boils at 250 K, and auto-ignites at 858 K; it has flammability limits in air of 3.9 % by volume to 74 % by volume. Its viscosity is 8.79 µPas at 1 bar and 20°C, it has an octane number of 131.

Table 1. Engine Specification

Engine type	Four stroke, single cylinder, water cooled direct injection diesel engine
Piston type	Bowl-in-piston
Capacity	661 cm^3
Maximum power / HP	5.5 KW / 7.3 HP at 1500 rpm
Maximum torque	35 Nm
Bore × Stroke	87.5 mm × 110 mm
Compression ratio	17.5:1
Speed	1500 rpm
Fuel blend	Diesel, PJB20 and PJB20 + hydrogen
Percentage Load	25, 50 and 100
Injection timing	23.4^0 Btdc
Injection Pressure	240 bar
Type of fuel injection	Pump-in-line injection system
No. of nozzle holes	3, 4, 5

2.1. Response surface methodology

Response Surface Methodology uses structured experiments to determine the appropriate response to many explanatory variables and one or more response variables. Although an approximation, Box and Wilson suggested employing a second-degree polynomial model since it is easy to estimate and use even with limited process understanding. RSM is commonly employed to optimize operational factors for maximizing the production of specific substances. Recently, RSM has been widely used for formulation optimization with well-designed experiments. Box–Behnken designs, created by George E. P. Box, are specific experimental designs utilized in RSM. This study aims to model and predict the output responses of an RSM experimental process, specifically focusing on brake thermal efficiency, brake specific fuel consumption, CO, HC, NOx, and smoke emissions. Experiments were analyzed using a second-order polynomial model and regression. This polynomial equation linked input and output reactions mathematically. Model-fitted response surface plots showed projected output responses.

Experiments were planned using selected levels of fuel blend, engine load, and the number of nozzle holes as input variables. The final step involved generating response plots with fit models to display the anticipated output responses. This model examines every possible operating state of the yield and is based on the quadratic equation:

$$Z = M_0 + M_1 A + M_2 B + M_{12} AB + M_{11} A_2 + M_{22} B_2 \quad (1)$$

Z is the Output response. A and B are independent operating variables, M_0 is constant. The linear terms' coefficients are M_1 and M_2. The interaction term coefficient is M_{12}. Quadratic term coefficients are M_{11} and M_{22}. The model was tested using analysis of variance after the experiment. ANOVA helps determine model significance and the effect of linear, interaction, and square terms on response Z. Optimization was done using response surface methodology's desirability approach. The response values are scaled to a desirability scale from 0, indicating complete undesirability, to 1, indicating high desirability. Finding A and B levels that enhance desirability is the goal. An ideal solution has the maximum

desirability. The approach determines the optimal operating parameters for the best reaction, Z.

2.2. Uncertainty analysis for experiments

The exhaust gas emissions measurement and performance parameter computation uncertainties are shown in **Table 2**. When determining the uncertainty of parameters that have been assessed based on two or more independent parameters

$$\frac{Uy}{Y}=\sqrt{\left(\frac{Ux1}{x1}\right)^2+\left(\frac{Ux2}{x2}\right)^2+\left(\frac{Uxn}{xn}\right)^2} \quad (1)$$

The uncertainty Uy and the testing value Y are respectively obtained from the evaluated parameters X_1, X_2, ...Xn.

Uncertainties in performance parameters are calculated as given below,

Uncertainty in Brake power,

$$\frac{\Delta BP}{BP}=\sqrt{\left(\frac{\Delta N}{N}\right)^2+\left(\frac{\Delta W}{W}\right)^2} \quad (a)$$

Uncertainty in Brake thermal efficiency,

$$\frac{\Delta BTE}{BTE}=\sqrt{\left(\frac{\Delta BP}{BP}\right)^2+\left(\frac{\Delta mf}{mf}\right)^2} \quad (b)$$

Uncertainty in specific fuel consumption,

$$\frac{\Delta SFC}{SFC}=\sqrt{\left(\frac{\Delta mf}{mf}\right)^2+\left(\frac{\Delta BP}{BP}\right)^2} \quad (c)$$

Measured exhaust emission values are subject to uncertainty based on the measurement range and resolution of the instrument for each emission component, and the values are calculated and expressed as follows: HC = ±0.005%, O_2 = ±0.04%, CO = ±0.1%, CO_2 = ±0.5%, NO_x = ±0.00011% respectively.

Table 2 Experimental uncertainties

Parameters	BP	BTE	Pressure	TFC	SFC	EGT	NOx	CO	CO_2	HC
% uncertainty	±2.01	±2.10	±0.14	±0.669	±2.11	±0.25	±0.0001	±0.1	±0.5	±0.0005

In order to calculate the overall uncertainty of an experiment, one must add the uncertainties of each instrument and this is what is shown below.

The total percentage of experiment uncertainty,

$$\sqrt{\left(\frac{\Delta BTE}{BTE}\right)^2+\left(\frac{\Delta \mathrm{TFC}}{\mathrm{TFC}}\right)^2+\left(\frac{\Delta SFC}{SFC}\right)^2+\left(\frac{\Delta BP}{BP}\right)^2+\left(\frac{\Delta CO}{CO}\right)^2+\left(\frac{\Delta HC}{HC}\right)^2+\left(\frac{\Delta NOX}{NOX}\right)^2+\left(\frac{\Delta P}{P}\right)^2+\left(\frac{\Delta EGT}{EGT}\right)^2}$$

$$\sqrt{(0.0210)^2+(0.0069)^2+(0.0211)^2+(0.02)^2+(0.001)^2+(0.00005)^2+(0.000001)^2+(0.0014)^2+(0.0025)^2}$$

$$=\pm 3.664\%$$

3. Result and discussion

The study focused on analyzing efficiency and emissions using Design Expert software to develop quadratic models. Experimental plans were meticulously crafted to construct these models, followed by rigorous data collection. ANOVA played a pivotal role in evaluating the significance of the regression models, individual coefficients, and assessing lack of fit. The ANOVA outcomes provided valuable insights across multiple parameters. For brake thermal efficiency, significant influencing variables were identified, and overall model significance was evaluated. Regarding BSFC, critical factors affecting fuel consumption were pinpointed, and model adequacy was assessed. Similarly, for CO, HC, NOx emissions, and smoke emissions.

ANOVA identified influential predictors and evaluated model performance. Utilizing Design Expert and ANOVA, the study summarized the significance of the regression models for each output variable. This comprehensive analysis, leveraging F-values, P-values, and lack of fit tests, clarified the factors impacting performance and emissions. It guided optimization efforts and improvements in experimental setups to enhance efficiency and reduce emissions. Detailed ANOVA tables and results from Design Expert would provide deeper insights, confirming the significance of variables and validating the quadratic models developed for each parameter as illustrated in **Table 3**.

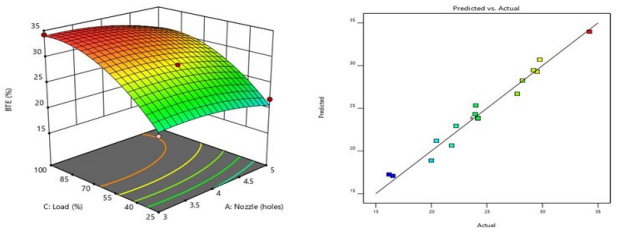

(a) BTE - Output Response (b) Predicted vs Actual

Figure 2. Response Surface for brake thermal efficiency

3.1. Response surface of brake thermal efficiency, BSFC, NOx, CO, HC and smoke:

3.1.1. Response surface for brake thermal efficiency

Figure (2) shows the analysis of BTE with respect to nozzle configuration, fuel blend ratio and engine load. Data was extracted for the BTE for different numbers of nozzle configuration with either 3, 4, or 5 holes, with a fuel blend ratio of diesel and PJB20 with hydrogen at 6 LPM and an engine load condition of 25%, 50% and 100%. It is observed that the combination of the 4-hole nozzle with PJB20 hydrogen fuel blend at 50% engine load generates the optimized BTE of 28.5% while the percentage

variation between predicted and experimental values comes out to be 1.05%. The results show that with a higher ratio of hydrogen, 6 LPM, in PJB20 blend, the BTE increases, likely as a result of improved penetration and finer droplet size, hence facilitating mixing with air. Increment of injector nozzle holes from 3 to 5 at full load condition tends to maximize fuel entry into the combustion chamber and increases the spray penetration hence enhancing thermal efficiency. **Figure (2a)** shows the comparison in experimental actual output response. **Figure (2b)** indicates that experimental and actual values correlate well. Better match was achieved with 0.9734 correlation coefficient. Due to optimal air-fuel combination in the combustion chamber, higher blend B20 improves BTE with their load

Table 3 Design Matrix

Run Order	Factor 1 A: Nozzle (holes)	Factor 2 B: Fuel blend (%)	Factor 3 C: Load (%)	Response 1 BTE (%)	Response 2 BSFC (kg/kw-hr)	Response 3 NO_x (ppm)	Response 4 HC (ppm)	Response 5 CO (%)	Response 6 Smoke (%)
1	4	20	25	16.2	0.56	114	29	0.04	20.1
2	3	10	25	22.23	0.39	339	58	0.072	23.4
3	4	20	50	28.5	0.25	120	29	0.2	30.3
4	4	20	50	28.5	0.25	120	29	0.2	30.3
5	4	20	100	28.2	0.27	132	29	0.91	66.3
6	5	0	25	16.54	0.483	112	27	0.04	18.9
7	4	10	50	29.51	0.27	975	67	0.049	29.3
8	5	20	50	20.46	0.324	109	39	0.3	50.2
9	5	0	100	27.73	0.288	123	27	0.24	58.2
10	3	10	100	34.22	0.25	2277	100	0.164	59.8
11	4	20	50	28.5	0.25	120	29	0.09	30.3
12	3	20	50	23.95	0.272	101	48	0.033	73.3
13	3	0	100	29.19	0.272	148	43	0.22	45.6
14	4	20	50	28.5	0.25	120	29	0.2	30.3
15	4	20	50	28.5	0.25	120	29	0.2	30.3
16	4	20	50	28.5	0.25	120	29	0.2	30.3
17	5	10	25	21.83	0.4	479	48	0.073	25.1
18	4	0	50	24	0.33	121	24	0.079	25.4
19	5	10	100	29.76	0.27	882	158	1.795	66.9
20	3	0	25	20	0.461	131	11	0.05	15.6

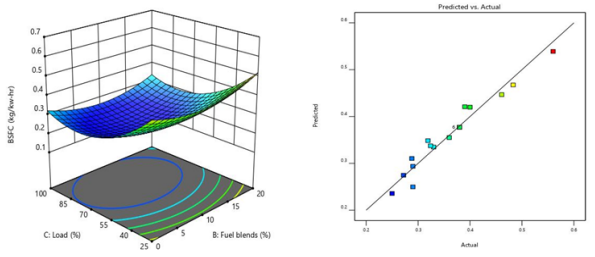

(a) BSFC - Output Response (b) Predicted vs Actual

Figure 3. Response Surface for brake specific fuel consumption

3.1.2. Response surface for brake specific fuel consumption

In dual-fuel mode using hydrogen 6 LPM and biodiesel blends PJB20, diesel, the number of holes in the injector nozzle has a great effect on brake specific fuel consumption shown in **Figure (3)**. However, generally speaking, a 3-hole injector usually gives a higher BSFC due to larger droplets and less efficient mixing. A 4-hole injector will yield better atomization and mixing for a lower BSFC. so 5-hole injector gives the best atomization and is therefore able to bring out the most efficient combustion with the lowest BSFC. BSFC at 50% load was found to be 0.272 for the 3-hole nozzle at 6 LPM blend which is the smallest, compared to 0.275 for the Diesel, 0.36 Kg/kw-h for the PJB20 fuel blend, also 0.33, 0.27, and 0.25 Kg/kw-h for the 4-hole nozzle (Diesel, PJB20, H_2 at 6 LPM) for three fuel blends of higher fuel distribution and combustion efficiency due to increased injector holes reduce BSFC. Then also 0.288, 0.29, and 0.324 Kg/kw-h for the 5-hole nozzle where further increasing due to increased the injector hole number. Hydrogen can improve biodiesel combustion by offering easier ignition of the fuel mixture. This, in turn, can provide more complete combustion with reduced unburned fuel and lower BSFC. An optimal blend will balance out the fast combustion characteristics of hydrogen with the stable combustion properties of biodiesel, leading to improved efficiency. Proper timing ensures that hydrogen has mixed well with the air before combustion. **Figure (3a)** depict the comparison in experimental actual output response. **Figure (3b)** the correlation between experimental and actual values is nearly perfect. The correlation coefficient is 0.9473, which fits better. Increased oxygen content in diesel blends promotes complete fuel combustion and improved BSFC

3.1.3. Response Surface for CO and HC emissions

The **Figure (4)** indicates the CO and HC analysis with respect to nozzle configuration, fuel blend ratio, and engine load. The variation of a number of nozzle holes significantly affects the formation of HC and CO emissions in dual-fuel mode. A number of nozzle holes were requisites in order to achieve air-fuel with complete combustion for proper break-up into finer fuel droplets that vaporize. PJB20 and 6 LPM of hydrogen leads to a homogenous charge, alleviate combustion will significantly reduces CO and HC, compared to diesel and PJB20. The HC emission has optimum for 4 hole nozzle related with 3 and 5 for PJB20 at 6 LPM compared to PJB20 and diesel for a middle load as 29 ppm with 0.21% for 4 hole, 100 ppm with 0.91% for 3 hole, 158 ppm with 1.79% for 5 hole respectively. CO emission levels obtained optimum for H_2 at 6 LPM nozzle hole of 3, 4 and 5 were 0.27, 0.24 and 0.26% compared to 0.29% for neat diesel operation with 3 hole nozzle injector. Due to biodiesel blends' increased combustion efficiency because of higher cetane number and oxygen content, and the injection of hydrogen along with PJB20, which will increase the combustion by the clean burning properties of hydrogen and higher flame speed, leading to leaner air fuel mixtures and complete oxidation of hydrogen and carbon. **Figure (4a & 4c)** shows the comparison in experimental actual output response. **Figure (4b & 4d)** the graph shows a strong correlation between the experimentally obtained and real values. This proves correct with very minor error, further proving that the correlation coefficients attained are 0.887 and 0.8846 with a better fit.

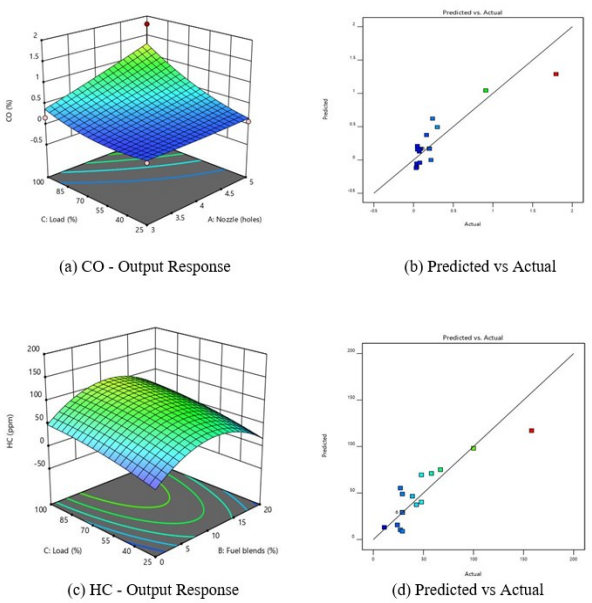

(a) CO - Output Response (b) Predicted vs Actual

(c) HC - Output Response (d) Predicted vs Actual

Figure 4. Response Surface for CO and HC emissions

3.1.4. Response Surface for NO_X emission

The NOx emissions from diesel engines are mainly controlled by combustion temperature and the availability of oxygen during the combustion process. With high temperatures, there will be increased formation of NOx emission nitrogen and oxygen in air react under thermal conditions. Variation of a number of nozzles holes from 3, 4, and 5 for diesel, PJB20, and PJB20 with hydrogen gas 6 LPM was shown in **Figure (5)**. It ensures variations in the number of nozzle holes that PJB20 and hydrogen gas is well dispersed in the combustion chamber to strike on combustion efficiency and uniformity of fuel distribution. At middle load conditions with PJB20 and 6 lpm, the lowest NOx emissions of 101 ppm, while the highest NO_X emissions of 2277 ppm were obtained. The NOx emission obtained for PJB20 fuelled with H_2 at 6 LPM at nozzle hole 3, 4 and 5 were 101, 120 and 109 ppm compared with 98 ppm for neat diesel operation with 3 hole nozzle. However, 4 hole nozzle of PJB20 fuelled with H_2 at 6 LPM injector nozzle emitted more NOx from the tail pipe. The high flame speed and wide flammability limitations of hydrogen improve uniform burning and reduce soot and incomplete combustion products associated with NOx emissions. **Figure (5a)** – compare experimental actual output response. **Figure (5b)** shows that experimental and actual values are correlated correctly with very minimal error. The achieved correlation coefficient was 0.8628, which is a better fit. Upper loads were the ones that showed the most significant increase in NOx

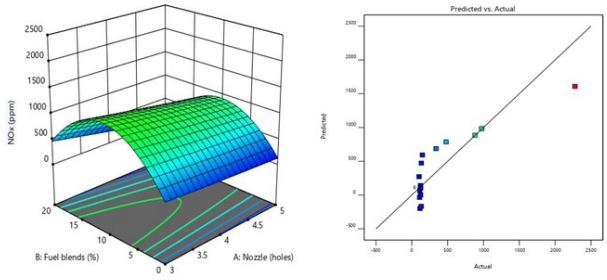

(a) NOx - Output Response (b) Predicted vs Actual

Figure 5. Response Surface for NOX emission

3.1.5. Response surface for smoke opacity

The smoke opacity for neat diesel, PJB20, and PJB20 with 6 lpm hydrogen across 3-hole, 4-hole, and 5-hole injectors generally showed that an increase in the number of holes reduces smoke opacity. As shown in the **Figure (6)**, the smoke opacity is high because of poor atomization from a 3-hole injector for neat diesel. A 4-hole injector reduces smoke opacity somewhat by improving fuel mixing; a 5-hole injector continues to reduce the smoke opacity even further. The increase of biodiesel's viscosity is what makes smoke opacity increase in the case of a 3-hole injector like PJB20. This is reduced using 4-hole and, in particular, 5-hole injectors. The 5-hole injector provides the lowest smoke opacity since it obtains superior atomization as well as efficient fuel-air mixing; hydrogen will be useful to attain cleaner combustion. It has generally been found that the smoke opacity increases with the increase in the number of injector nozzles used from 3 to 5. A percentage decrease of 4 hole nozzle is 10.61% is found at middle load use for JB20 + H_2 6 LPM when compared with diesel and PJB20 were to be optimized. Especially, this trend is very important for the reduction of particulate emissions in a cleaner operation when blending hydrogen into biodiesel. In the obtained experimental actual output response comparison graph in **Figure (6a)**, there is no overlap in experiments; the experimental and actual values came near in **Figure (6b)**, which can denote a good

fit regarding correlation. Found correlative coefficient by the value 0.9189, by that, the fit is quite good.

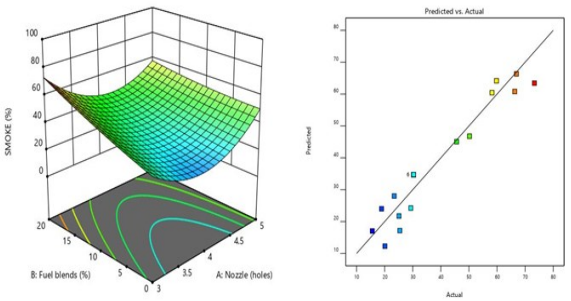

(a) Smoke - Output Response (b) Predicted vs Actual

Figure 6. Response Surface for Smoke emission

3.1.6. Analysis of model

Brake Thermal Efficiency: The Model F-value of 40.64 indicate that the quadratic model is statistically considerable for predict brake thermal efficiency. This means there is only a 0.01% chance that such a large F-value could occur due to random noise in the data. Significant model terms include A, C, B^2, and C^2 ($P < 0.0500$), indicating that these variables have a significant impact on brake thermal efficiency. Variables A and C likely represent factors such as fuel blend or engine load, while B^2 and C^2 denote quadratic effects, suggesting nonlinear relationships that affect efficiency. The suggestion to consider model reduction implies that eliminating non-significant terms (those with P-values greater than 0.1000) could improve the precision of the model by focusing on the most influential factors.

BSFC (Brake Specific Fuel Consumption): The Model F-value of 19.98 shows that the quadratic model is statistically significant for BSFC, with a very low chance (0.01%) of such a large F-value occurring due to noise. Significant model terms identified are B, C, B^2, and C^2 ($P < 0.0500$). These terms indicate that variables B and C, possibly related to engine load or injector configuration, and their quadratic effects (B^2 and C^2) play a crucial role in determining BSFC. The suggestion to simplify the model by removing non-significant terms aims to enhance its accuracy in predicting fuel consumption under varying conditions.

NOx Emission: The Model F-value of 3.57 indicates statistical significance, with a 2.99% chance of occurring due to noise. The significant model term identified is B^2 ($P < 0.0500$), suggesting that the quadratic effect of variable B (likely an operational parameter such as engine load or injection timing) strongly influences NOx emissions. This finding highlights the importance of considering nonlinear relationships in predicting and controlling NOx levels in diesel engines.

HC Emission: The Model F-value of 4.05 shows statistical significance, with a 1.99% chance of occurring due to noise. Significant model terms comprise C and B^2 ($P < 0.0500$), signifying that variables C number of nozzle hole or fuel blend and the quadratic effect of B are important predictors of HC emissions. This suggests that engine operational factors and their interactions significantly impact hydrocarbon emissions, influencing emissions control strategies.

CO Emission: The Model F-value of 4.11 designate statistical significance, with a 1.90% chance of going on due to noise. Significant model terms identified are A, C, and AC ($P < 0.0500$), suggesting that variables A (possibly related to combustion parameters or fuel blend), C (injector configuration or operational settings), and their interaction of AC have a significant influence on CO emissions. The significant Lack of Fit (F-value of 66.13) indicates that the model may need enhancement to better fit the data and improve its analytical ability for CO emissions.

Smoke Emission: The Model F-value of 12.59 indicates statistical significance, with a very low chance (0.02%) of occurring due to noise. Significant model terms include B, C, and A^2 ($P < 0.0500$), highlighting the significance of variables B (perhaps associated to injector configuration and engine load or), C (operational parameters), and the quadratic effect of A in predicting smoke emissions. This implies that optimizing these factors can lead to reduced smoke emissions from the engine, benefiting both performance and environmental considerations. **Table 4** shows the regression equations obtained from the analysis of variance (ANOVA).

Table 4. Regression equation

BTE = +31.41-1.39 A -0.6746 B +5.28 C -0.2532 AB -0.2426 AC +0.2262 BC -1.07 A^2 -4.71 B^2 -3.27 C^2 **BSFC** = +0.2518 + 0.0033A + 0.0190B -0.0888C -0.0108AB +0.0038AC- 0.0065BC-0.0309A^2 + 0.0623B^2 + 0.1107 C^2
NOx = +1078.83 - 156.06A +11.39B + 254.81C - 66.22 AB -205.77AC +80.55BC +8.87A^2 -857.38B^2 - 95.53C^2
HC = +82.22 + 4.35A +7.12B +18.67C + 0.5197AB +5.14AC +1.36BC +14.38A^2 -52.77B^2-7.64C^2
CO = 0.3066 + 0.2349A + 0.1726B + 0.3460C + 0.1458AB + 0.2219AC + 0.2032BC + 0.0180A^2-0.1457B^2 + 0.1613C^2
Smoke = +31.75 -1.02 A +10.14 B +20.18 C -6.61 AB +2.11 AC +4.07 BC +20.37 A^2 +1.71 B^2-7.05 C^2

Table 5. Model evaluation

Model	BTE	BSFC	NOx	HC	CO	SMOKE
Mean	24.45	0.3649	338.15	44.1	0.2578	38
SD	0.99	0.023	33.9	21.16	0.096	7.05
R^2 (%)	0.9734	0.9473	0.8628	0.8846	0.887	0.9189
Model type	Quadratic	Quadratic	Quadratic	Quadratic	Quadratic	Quadratic
Adj. R^2 (%)	0.9494	0.899	0.8493	0.8608	0.8554	0.846
Pred. R^2 (%)	0.956	0.923	0.855	0.876	0.864	0.896

3.1.7. Model evaluation of model

ANOVA results from **Table 5** assess BTE, BSFC, NOx, HC, CO, and Smoke model have predicted R^2 values of 0.956, 0.923, 0.855, 0.876, 0.864, and 0.896, with their adjusted R^2 values. Most cases show a discrepancy between Predicted R^2 and Adjusted R^2 of less than 0.2, indicating close alignment and no severe issues with the model or data. This model is good and will navigate design with satisfactory outcomes because its signal-to-noise ratio precision is more than four. Model stability was validated by p values below 0.0001. Regression statistics include R^2 and Adjusted R^2, which are in agreement. Adjusted R^2 considers the number of predictors in the model, while R^2 evaluates response variability with significant factors. Generally, high R^2 and Adjusted R^2 values indicate a well-fitting model. The accuracy, R^2, Adjusted R^2, and Predicted R^2 near RSM optimization approach are within specified limitations.

3.1.8. Optimization criteria

Table 6 shown the RSM methodology was implemented to optimize various parameters like nozzle hole size, fuel blend and load in engine operations. The multi-response optimization was performed to maximize BTE and to minimize BSFC, NOx, HC, CO and Smoke. In the desirability approach, 3 was set as the highest priority to performance and emission responses for BTE, BSFC, NOx, HC, CO and Smoke. Few of the best solutions exhibited maximum desirability and were favored. A desirability score of 0.998 was the maximum obtained with a four-hole nozzle, B20 fuel blend along with H_2 at 6 LPM, and a 50% load. As per reference, those solutions where the desirability is maximum are the optimal solutions.

3.1.9. Validation experiments

Additional tests were conducted in order to determine the optimum conditions for a four-hole nozzle, a JB20 fuel blend with Hydrogen at 6 LPM flow rate, and a 50% load. Three repeated tests proved these measured response values to be very close to the predicted response values, hence affirming the accuracy of the models, since there is strong agreement between the predicted and experimental results as shown in **Table 7**.

Table 6 Optimization Criteria

Source	Lower limits	Upper limits	Importance	Goal	Desirability
Nozzle	3	5	3	is in range	1
Fuel blend	0	20	3	is in range	1
Load	25	100	3	is in range	1
BTE	16.2	34.22	3	Maximize	0.998
BSFC	0.25	0.56	3	Minimize	0.867
NOx	101	2277	3	Minimize	0.868
HC	11	158	3	Minimize	0.865
CO	0.033	1.795	3	Minimize	0.889
Smoke	15.6	73.3	3	Minimize	0.869

Table 7. Validation Experiments

Optimized Parameters			Value	B_{th} (%)	BSFC (kg/kw-hr)	Nox (ppm)	HC (ppm)	CO (%)	Smoke (%)
Nozzle (holes)	Fuel Blend (%)	Load (%)							
4	20	50	Predicted	29.55	0.276	135	32	0.26	45.1
			Actual	28.5	0.25	120	29	0.20	30.3
			Error	1.05	0.026	15	3	0.06	14.8

4. Conclusion

This study examines the performance and emission characteristics of Homogeneous Charge Compression Ignition (HCCI) engines using diesel, biodiesel, and a blend of Juliflora Biodiesel (B20) with hydrogen at 6 LPM in dual-fuel mode. ANOVA fulfilled several critical roles in the analysis.

- Firstly, it tested the adequacy of the quadratic regression models to ensure they accurately represented the relationships between variables, with a significant F-value indicating strong model fit.
- Secondly, ANOVA identified statistically significant coefficients (variables) in the models, typically those with P-values less than 0.05. Lastly, it assessed lack of fit to determine if the models adequately captured the experimental data, where a non-significant lack of fit indicated satisfactory model performance.
- The experimental results indicated that a 4-hole nozzle at 50% load (B20 + H2 @ 6 LPM) provided superior atomization with increased efficiency and nitrous oxide, along with reduced CO, HC, and smoke emissions compared to the 3 hole and 5 hole nozzles.
- Additional tests were conducted in order to determine the optimum conditions for a four-hole nozzle, a JB20 fuel blend with Hydrogen at 6 LPM flow rate, and a 50% load.
- Response surface methodology confirmed that these experimental findings align with optimized parameters. Therefore, we recommend using a 4-hole nozzle for the B20 + H_2 blend at 6 LPM and 50% load to achieve enhanced performance and emission

reductions in HCCI engines compared to 3-hole and 5-hole nozzles.

References

Allasi H.L., Rajalingam A., Jani S.P.and Uppalapati S. (2023). Influence Of Synthesized (Green) Cerium Oxide Nanoparticle With Neem (Azadirachta Indica) Oil Biofuel. *Bulletin of the Chemical Society of Ethiopia*, **37**(2), 477–490, https://doi.org/10.4314/bcse.v37i2.16

Atmanli A., Yuksel B., Ileri E. and Karaoglan A.D. (2015). Response surface methodology based optimization of diesel-n-butanol cotton oil ternary blend ratios to improve engine performance and exhaust emission characteristics. *Energy Conversion and Management*, **90**, 383–394. https://doi.org/10.1016/j.enconman.2014.11.029

Bhagat R.N., Sahu K.B., Ghadai S.K., Kumar C.B. (2023). A review of performance and emissions of diesel engine operating on dual fuel mode with hydrogen as gaseous fuel, *International Journal of Hydrogen Energy*, **48**(70), 27394–27407. https://doi.org/10.1016/j.ijhydene.2023.03.251.

Bora B.J., Dai Tran T., Shadangi K.P., Sharma P., Said Z., Kalita P., Buradi A., Nguyen V.N., Niyas H., Pham M.T., Le C.T.N., Tran V.D. and Nguyen X.P. (2022). Improving combustion and emission characteristics of a biogas/biodiesel-powered dual-fuel diesel engine through trade-off analysis of operation parameters using response surface methodology, Sustainable Energy Technologies and Assessments, **53**, Part A, 2022, 102455. https://doi.org/10.1016/j.seta.2022.102455.

Botla G., Barmavatu P. and Pohorely M. (2024). Michal Jeremias, Vineet Singh Sikarwar, Optimization of value-added products using response surface methodology from the HDPE waste plastic by thermal cracking, *Thermal Science and Engineering Progress*, **50**, 102514, https://doi.org/10.1016/j.tsep.2024.102514.

Deheri C., Acharya S.K., Thatoi D.N. and Mohanty A.P. (2020) A review on performance of biogas and hydrogen on diesel engine in dual fuel mode, *Fuel*, **260**, 116337.

Gerhard K. (2005). Dependence of biodiesel fuel properties on the structure of fatty acid alkyl esters, Fuel Processing Technology, **86**, (10), 1059–1070. https://doi.org/10.1016/j.fuproc.2004.11.002.

Halewadimath S.S., Banapurmath N.R., Yaliwal V.S., Gaitonde V. N., Khan T.Y., Vadlamudi C., Krishnappa S.and Ashok M. (2023). Sajjan Experimental Investigations on Dual-Fuel Engine Fueled with Tertiary Renewable Fuel Combinations of Biodiesel and Producer-Hydrogen Gas Using Response Surface Methodology, Sustainability 2023, 15, 4483. https://doi.org/10.3390/su15054483

Hosseini S.H., Tsolakis A., Alagumalai A., Mahian O., Lam S.S., Pan J., Peng W., Tabatabaei M. and Aghbashlo M. (2023). Use of hydrogen in dual-fuel diesel engines. *Progress in Energy and Combustion Science*, **98**, 101100. https://doi.org/10.1016/j.pecs.2023.101100.

Karagöz Y, Sandalcı T, Yüksek L, Dalkılıo AS, Wongwises S. Effect of hydrogen–diesel dual-fuel usage on performance, emissions and diesel combustion in diesel engines. Advances in Mechanical Engineering. 2016, 8(8). doi:10.1177/1687814016664458

Karin P., Tripatara A., Wai P., Oh B.S., Charoenphonphanich C., Chollacoop N. and Kosaka H. (2022). Influence of ethanol-biodiesel blends on diesel engines combustion behavior and particulate matter physicochemical characteristics. *Case Studies in Chemical and Environmental Engineering*, 6, 100249. https://doi.org/10.1016/j.cscee.2022.100249.

Khan M.I. and Akhtar N. (2012). Hydrogen-Biodiesel Dual Fuel Mode: Performance and Emission Characteristics. *International Journal of Hydrogen Energy*, **37**(7), 6001–6009.

Khan O., Alsaduni I., Equbal A., Parvez M. and Yadav A.K. (2024). Performance and emission analysis of biodiesel blends enriched with biohydrogen and biogas in internal combustion engines. Process Safety and Environmental Protection, **183**, 2024, 1013–1037. https://doi.org/10.1016/j.psep.2024.01.049.

Kishore N.P., Gugulothu S.K., Reddy R.V. and Barmavatu P. (2024). Trade-off study on environmental aspects of a reactivity controlled compression ignition engine using 1-hexanol and jatropha oil/diesel in dual fuel mode, *Applied Thermal Engineering*, **246**, 122891. https://doi.org/10.1016/j.applthermaleng.2024.122891

Mittelbach M. and Schober S. (2003). Biodiesel Production and Properties. Biodiesel Handbook, 1st Edition.

Mohamed M.F., Jegan N., Prabhu V.M., Ranjith R. and Priyan T.V. (2021). Optimization of performance and emission characteristics of VCR engine with biodiesel using response surface methodology, *Materials Today: Proceedings*, **39**, Part 1, 2021, 77–83. https://doi.org/10.1016/j.matpr.2020.06.161

Mohite A., Bora B.J., Sharma P., Sarıdemir S., Mallick D., Sunil S and Ağbulut U. (2024). Performance enhancement and emission control through adjustment of operating parameters of a biogas-biodiesel dual fuel diesel engine: An experimental and statistical study with biogas as a hydrogen carrier, International Journal of Hydrogen Energy, **52**, Part A, 2024, 752–764. https://doi.org/10.1016/j.ijhydene.2023.08.201.

Najafi G., Ghobadian B., Yusaf T., Ardebili S.M.S. and Mamat R. (2015). Optimization of performance and exhaust emission parameters of a SI (spark ignition) engine with gasoline-ethanol blended fuels using response surface methodology. *Energy*, **90**, 1815–1829.

Nayak S.K. and Mishra P.C. (2019). Combustion characteristics, performances and emissions of a biodiesel-producer gas dual fuel engine with varied combustor geometry, *Energy*, **168**, 585–600. https://doi.org/10.1016/j.energy.2018.11.116.

Parimi K.B., Kaur B.S., Lankapalli S.V.P. *et al.* (2023). Performance, combustion, and emission characteristics of on a diesel engine fuelled with hydrogen compressed natural gas and Kusum seed biodiesel. Waste Dispos. *Sustainable. Energy* 5, 151–163. https://doi.org/10.1007/s42768-022-00132-0

Pullagura G., Vanthala V.S., Vadapalli S., Bikkavolu J.R., Barik D., Sharma P., Bora B.J. (2024). Enhancing performance characteristics of biodiesel-alcohol/diesel blends with hydrogen and graphene nanoplatelets in a diesel engine. *International Journal of Hydrogen Energy*, **50**, Part B, 2024, 1020–1034. https://doi.org/10.1016/j.ijhydene.2023.09.313

Rajesh S.P., Retnam B.S.J., Devanand M., Lenin A.H. and Manjunathan A. (2022). Performance Analysis on PP blended Bio-Diesel tested on a CI Engine. *International Journal of*

Vehicle Structures and Systems, **14**(3), 333–335, https://doi.org/10.4273/ijvss.14.3.09

Rajesh S.P., Retnam B.S.J., Dhas J.E.R., Lenin A.H. and Manjunathan A. (2022). Specific Fuel Consumption and Exhaust Emission Test on Single Cylinder Four-Stroke Diesel Engine using Polyethylene Extract Biodiesel as Fuel. *International Journal of Vehicle Structures and Systems*, **14**(3), 339–341, https://doi.org/10.4273/ijvss.14.3.11

Rex P., Rahiman M.K., Barmavatu P., Aryasomayajula Venkata Satya Lakshmi S.B. and Meenakshisundaram N. (2024). Catalytic pyrolysis of polypropylene and polyethylene terephthalate waste using graphene oxide-sulfonated zirconia (GO-Szr) and analysis of its oil properties for Bharat Stage VI fuel production, *Environmental Quality Management*, **33**(4), 2024, 501–511. https://doi.org/10.1002/tqem.22106

Rorimpandey P., Yip H.L., Srna A., Zhai G., Wehrfritz A., Kook S., Hawkes E.R. and Chan Q.N. (2023). Hydrogen-diesel dual-fuel direct-injection (H2DDI) combustion under compression-ignition engine conditions, *International Journal of Hydrogen Energy*, **48**(2), 766–783. https://doi.org/10.1016/j.ijhydene.2022.09.241.

Sagari J.K., Kaur B.S., Vadapalli S., Dadi V.T., Guddanti S.S. and Lakkoju S.K. (2020). Comprehensive performance, combustion, emission`, and vibration parameters assessment of diesel engine fuelled with a hybrid of niger seed oil biodiesel and hydrogen: response surface methodology approach. *SN Applied Sciences*, **2**(9), https://doi.org/10.1007/s42452-020-03304-x

Santos M.C. and Oliveira F. (2011). Performance of Biodiesel-Ethanol Blends in Diesel Engines. *Energy Conversion and Management*, **52**(1), 123–129.

Saravanan N. and Nagarajan G. (2008). An experimental investigation of hydrogen-enriched air induction in a diesel engine system, *International Journal of Hydrogen Energy*, **33**(6), 1769–1775. https://doi.org/10.1016/j.ijhydene.2007.12.065.

Shajahan S., Gugulothu S.K., Muthyala R. and Barmavatu P. (2024). Role of different cavity flame holders on the performance characteristics of supersonic combustor, *International Journal of Turbo and Jet-Engines*. https://doi.org/10.1515/tjj-2024-0037

Shajahan S., Gugulothu S.K., Muthyala R., Barmavatu P. (2024). Numerical investigation on influence of different geometrical cavity flame holders and flame stabilization mechanism in hydrogen fueled multi-strut-based scramjet combustor, Proceedings of the Institution of Mechanical Engineers, Part E: *Journal of Process Mechanical Engineering*. doi:10.1177/09544089241286248

Sharma A., Ansari N.A., Pal A., Singh Y. and Lalhriatpuia S. (2019). Effect of biogas on the performance and emissions of diesel engine fuelled with biodiesel-ethanol blends through response surface methodology approach. *Renewable Energy*, **141**, 657–668.

Shrivastava K., Thipse S.S., Patil I.D. (2021). Optimization of diesel engine performance and emission parameters of Karanja biodiesel-ethanol-diesel blends at optimized operating conditions, *Fuel*, **293**, 120451. https://doi.org/10.1016/j.fuel.2021.120451.

Tutak W., Jamrozik A., Grab-Rogali ´nski K. (2023). Co-Combustion of Hydrogen with Diesel and Biodiesel (RME) in a Dual-Fuel Compression-Ignition Engine. *Energies* **16**, 4892. https://doi.org/10.3390/en16134892

Veza I., Spraggon M., Fattah I.R. and Idris M. (2023). Response surface methodology (RSM) for optimizing engine performance and emissions fueled with biofuel: Review of RSM for sustainability energy transition, *Results in Engineering*, **18**, 101213. https://doi.org/10.1016/j.rineng.2023.101213.

Wang S., Zhang Z., Hou X., Lv J., Lan G., Yang G. and Hu J. (2023). The environmental potential of hydrogen addition as complementation for diesel and biodiesel: A comprehensive review and perspectives, *Fuel*, **342**, 127794. https://doi.org/10.1016/j.fuel.2023.127794.

Wirawan S.S., Solikhah M.D., Setiapraja H., Sugiyono A. (2024). Biodiesel implementation in Indonesia: Experiences and future perspectives, Renewable and Sustainable Energy Reviews, **189**, Part A, 2024, 113911. https://doi.org/10.1016/j.rser.2023.113911.

Xu L., Dong H., Liu S., Shen L. and Bi Y. (2023). Study on the Combustion Mechanism of Diesel/Hydrogen Dual Fuel and the Influence of Pilot Injection and Main Injection. *Processes,* **11**, 2122. https://doi.org/10.3390/pr11072122.